

Strain-Controlled, Photochemically, or Thermally Promoted Haptotropic Shifts of Cyclopentadienyl Ligands in Group 8 Metallocenophanes

David E. Herbert, Makoto Tanabe,[†] Sara C. Bourke, Alan J. Lough,[‡]
and Ian Manners*

School of Chemistry, University of Bristol, Bristol, England, BS8 ITS

Received October 19, 2007; E-mail: ian.manners@bristol.ac.uk

Abstract: Cyclopentadienyl (Cp) ligands in moderately strained [1]- and [2]ferrocenophanes [Fe{(η⁵-C₅H₄)₂(ER_x)_y}: Fe{(η⁵-C₅H₄)₂SiMe₂} (**1**), Fe{(η⁵-C₅H₄)CH₂)}₂ (**10**)] and highly strained [2]ruthenocenophanes [Ru{(η⁵-C₅H₄)CR₂}₂ {R = H (**15**), Me (**16**)}] are susceptible to partial substitution by P donors and form mixed-hapticity metallocycles—[M(L₂){(η⁵-C₅H₄)(ER_x)_y(η¹-C₅H₄)}]: [Fe(dppe){(η⁵-C₅H₄)SiMe₂(η¹-C₅H₄)}] (**5**), [Fe(dmpe){(η⁵-C₅H₄)SiMe₂(η¹-C₅H₄)}] (**6**), [Fe(dmpe){(η⁵-C₅H₄)(CH₂)₂(η¹-C₅H₄)}] (**11**), [Ru(dmpe){(η⁵-C₅H₄)(CH₂)₂(η¹-C₅H₄)}] (**17**), [Ru(dmpe){(η⁵-C₅H₄)(CMe₂)₂(η¹-C₅H₄)}] (**18**), and [Ru(PMe₃)₂{(η⁵-C₅H₄)(CH₂)₂(η¹-C₅H₄)}] (**19**)—through haptotropic reduction of one η⁵-, π-bound Cp to η¹, σ-coordination. These reactions are strain-controlled, as highly ring-tilted [2]ruthenocenophanes **15** and **16** [tilt angles (α) ≈ 29–31°] react without irradiation to form thermodynamically stable products, while moderately strained [η]ferrocenophanes **1** and **10** (α ≈ 19–22°) require photoactivation. The iron-containing photoproducts **5** and **11** are metastable and thermally retroconvert to their strained precursors and free phosphines at 70 °C. In contrast, the unprecedented ring-opening polymerization (ROP) of the essentially ring-strain-free adduct **6** to afford poly(ferrocenyldimethylsilane) [Fe(η⁵-C₅H₄)₂SiMe₂]_n (M_w ≈ 5000 Da) was initiated by the thermal liberation of small amounts of P donor. Unlike reactions with bidentate analogues, monodentate phosphines promoted photolytic ROP of ferrocenophanes **1** and **10**. MALDI-TOF analysis suggested a cyclic structure for the soluble poly(ferrocenyldimethylsilane), **8-cyclic**, produced from **1** in this manner. While the polymer likewise produced from **10** was insoluble, the initiation step in the ROP process was modeled by isolation of a tris(phosphine)-substituted ring-opened ferrocenophane [Fe(PMe₃)₃{(η⁵-C₅H₄)(CH₂)₂(C₅H₅)}][OCH₂CH₃] (**13**[OCH₂CH₃]) generated by irradiation of **10** and PMe₃ in a protic solvent (EtOH). Studies of the cation **13** revealed that the Fe center reacts with a Cp[−] anion with loss of the phosphines to form [Fe(η⁵-C₅H₅){(η⁵-C₅H₄)(CH₂)₂(C₅H₅)}] (**14**) under conditions identical to those of the ROP experiments, confirming the likelihood of “back-biting” reactions to yield cyclic structures or macrocondensation to produce longer chains.

Introduction

The cyclopentadienyl anion and its derivatives (C₅H₅−*n*R_{*n*}; “Cp”) are widely used cyclic polyenyl π-ligands in organometallic complexes.¹ This popularity owes much to stable metal–Cp bonding and ancillary occupation of multiple coordination sites that allow selective chemistry to proceed in the remaining vacant coordination space at the metal center. Additionally, isomerization between geometrical bonding arrangements (illustrated in Figure 1), haptotropic shifts, can produce coordinative unsaturation and thereby enhance the reactivity of a metal complex.²

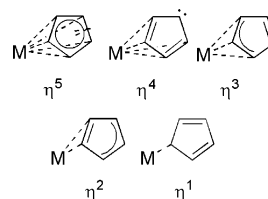


Figure 1. Representative bonding modes of the cyclopentadienide (Cp[−]) anion.

The tendency of complexes with metal–Cp bonds to engage haptotropic flexibility during associative substitution reactions is known to be amplified by electron-withdrawing substituents,^{3,4} and the most well-studied example, the “indenyl effect”, highlights how a π system contiguous to one or more of the Cp rings assists the ligand to seamlessly adjust to the electronic requirements of a metal center.⁵ Group 6 metallocene derivatives have also been shown to undergo well-characterized haptotropic shifts of Cp ligands.⁶

In d^x (x > 4) [η]metallocenophanes (or *ansa*-metallocenes), ring-strain increases the favorability of Cp ligand substitution

[†] Present address: Chemical Resources Laboratory, Tokyo Institute of Technology, 4259 Nagatsuta, Midori-ku, Yokohama 226-8503, Japan.

[‡] X-Ray Crystallography, Department of Chemistry, University of Toronto, 80 St. George Street, Toronto, Ontario, Canada, M5S 3H6.

(1) A recent publication cited that an estimated 80% of reported organometallic compounds contain cyclopentadienyl or derivative ligands. See: (a) Tamm, M.; Kunst, A.; Bannenberg, T.; Randoll, S.; Jones, P. G. *Organometallics* **2007**, 26, 417 and references therein. Metallocenes containing heteroatom-substituted Cp analogues (e.g., 1,2-diaza,3,5-diborolyl ligands) have also been reported. See, for example: (b) Ly, H. V.; Forster, T. D.; Parvez, M.; McDonald, R.; Roesler, R. *Organometallics* **2007**, 26, 3516.

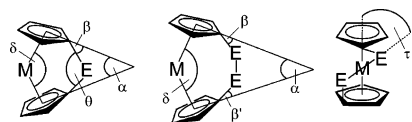
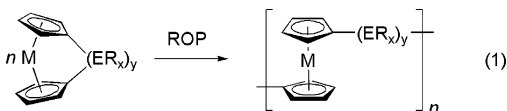
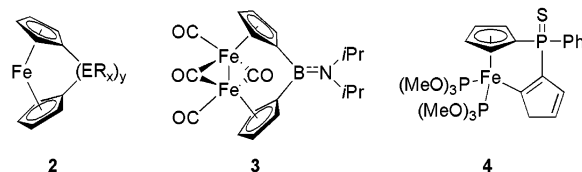


Figure 2. Definition of geometric parameters α , β , δ , θ , and τ in [1]- and [2]-bridged metallocenophanes. These angles become meaningful as qualitative measures of ring strain for d^x ($x > 4$) [n]metallocenophanes with short ($n \leq 2$) bridges.¹³

reactions as ring tilting significantly raises the free energy and weakens metal–Cp bonding.⁷ Nevertheless, in the wide range of strained metallocenophanes with different bridging elements,⁸ Cp ligands retain a strong preference for η^5 -Cp coordination, even with tilt angles (α , Figure 2) greater than 30° and β angles of up to 43° .⁹ Accordingly, the majority of the reactivity observed for these species involves polarized bonds between the *ipso* carbon and the bridging element. For example, ring-opening polymerization (ROP)¹⁰ (eq 1) of sila[1]ferrocenophanes ($\alpha \approx 19$ – 22° , $\beta \approx 37$ – 41°) initiated by anionic reagents such as $n\text{BuLi}$ ¹¹ or transition-metal catalysts¹² has been shown to proceed via C_{ipso} –Si bond cleavage.



In contrast, relatively few examples have been reported in which strain is relieved through breaking a metal–Cp bond. Highly strained, boron-bridged [1]ferrocenophanes [e.g., **2** ($\text{ER}_x)_y = \text{BN}(\text{iPr})_2$, $\alpha = 31^\circ$] undergo unexpected ring-opening chemistry involving an Fe–Cp bond on reaction with metal carbonyls, for example, $\text{Fe}_2(\text{CO})_9$, to yield bimetallic species **3**.¹⁴ Miyoshi and co-workers have shown that UV irradiation of phosphorus-bridged [1]ferrocenophanes **2** [$(\text{ER}_x)_y = \text{P}(\text{S})\text{-Ph}$] in the presence of phosphite ligands (e.g., $\text{P}(\text{OMe})_3$) yields the ring-slipped product **4**.¹⁵ Notably, mild photolytic ROP procedures for [1]ferrocenophanes initiated by substitution of one Cp ligand by moderate neutral^{15,16} or anionic¹⁷ bases have recently been described. The increasing importance of Group 8 and 9 [1]- and [2]metallocenophanes as precursors to high molecular weight functional metallopolymers through ROP¹⁰ has prompted our continued interest in their ring-opening chemistry.¹⁸



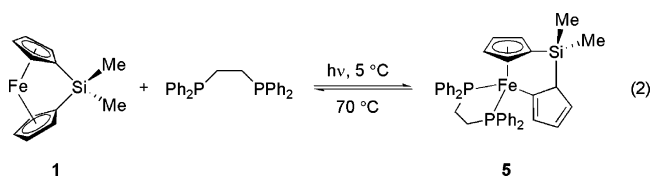
In this article, we report our detailed comparative studies¹⁹ of the photolytic and thermal reactivity of several [1]- and

- (2) For reviews of ring-slip chemistry, see: (a) O'Connor, J. M.; Casey, C. P. *Chem. Rev.* **1987**, *87*, 307. (b) Veiros, L. F. *Organometallics* **2000**, *19*, 5549. (c) McGlinchey, M. J. *Can. J. Chem.* **2001**, *79*, 1295. Regarding the role of haptotropic shifts in reaction mechanisms, see: (d) Rerek, M. E.; Ji, L. N.; Basolo, F. *Chem. Commun.* **1983**, 1208. (e) Rerek, M. E.; Basolo, F. *J. Am. Chem. Soc.* **1984**, *106*, 5908. (f) Simanko, W.; Sapunov, V. N.; Schmid, R.; Kirchner, K.; Wherland, S. *Organometallics* **1998**, *17*, 2391. (g) Simanko, W.; Tesch, W.; Sapunov, V. N.; Mereiter, K.; Schmid, R.; Kirchner, K.; Coddington, J.; Wherland, S. *Organometallics* **1998**, *17*, 5674. (h) Casey, C. P.; Clark, T. B.; Guzei, I. A. *J. Am. Chem. Soc.* **2007**, *129*, 11821. For theoretical treatments of haptotropic shifts in organometallic compounds, see: (i) Anh, N. T.; Elian, M.; Hoffmann, R. *J. Am. Chem. Soc.* **1978**, *100*, 110. (j) Albright, T. A.; Hoffmann, P.; Hoffmann, R.; Lillya, C. P.; Dobosh, P. A. *J. Am. Chem. Soc.* **1983**, *105*, 3396. (k) Romão, C. C.; Veiros, L. F. *Organometallics* **2007**, *26*, 1777.
- (3) (a) Sanderson, C. T.; Palmer, B. J.; Morgan, A.; Murphy, M.; Dluhy, R. A.; Mize, T.; Amstutz, I. J.; Kutal, C. *Macromolecules* **2002**, *35*, 9648. (b) Ding, W.; Sanderson, C. T.; Conover, R. C.; Johnson, M. K.; Amstutz, I. J.; Kutal, C. *Inorg. Chem.* **2003**, *42*, 1532. (c) Sanderson, C. T.; Quinlan, J. A.; Conover, R. C.; Johnson, M. K.; Murphy, M.; Dluhy, R. A.; Kutal, C. *Inorg. Chem.* **2005**, *44*, 3283. (d) Yamaguchi, Y.; Ding, W.; Sanderson, C. T.; Borden, M. L.; Morgan, M. J.; Kutal, C. *Coord. Chem. Rev.* **2007**, *251*, 515.
- (4) Slocum, D. W.; Beach, D. L.; Ernst, C. R.; Fellows, R.; Moronski, M.; Conway, B.; Bencini, J.; Siegel, A. *Chem. Commun.* **1980**, 1043.
- (5) (a) Decken, A.; Rigby, S. S.; Girard, L.; Bain, A. D.; McGlinchey, M. J. *Organometallics* **1997**, *16*, 1308. (b) Bradley, C. A.; Lobkovsky, E.; Keresztes, I.; Chirik, P. J. *J. Am. Chem. Soc.* **2005**, *127*, 10291. (c) Bradley, C. A.; Keresztes, I.; Lobkovsky, E.; Chirik, P. J. *Organometallics* **2006**, *25*, 2080.
- (6) For example, CrCp_2 reacts with nitric oxide to yield $\text{Cr}(\eta^5\text{-C}_5\text{H}_5)(\eta^1\text{-C}_5\text{H}_5)(\text{NO})_2$ at 0°C in solution, while reduction of $\text{W}(\text{Cp})_2\text{Cl}_2$ under a high pressure of CO yielded the unique mixed hapticity complex, $\text{W}(\eta^5\text{-C}_5\text{H}_5)(\eta^3\text{-C}_5\text{H}_5)(\text{CO})_2$, the first crystallographically characterized example of an η^3 -Cp ligand in a $\text{M}(\text{Cp})_2\text{L}_2$ complex. See: (a) Hames, B. W.; Legzdins, P.; Martin, D. T. *Inorg. Chem.* **1978**, *17*, 3644. (b) Wong, K. L. T.; Brintzinger, H. H. *J. Am. Chem. Soc.* **1975**, *97*, 5143. (c) Huttner, G.; Brintzinger, H. H.; Bell, L. G.; Friedrich, P.; Bejenke, V.; Neugebauer, D. *J. Organomet. Chem.* **1978**, *145*, 329. For other examples of haptotropic shifts of Cp ligands in group 6 metallocene derivatives, see: (d) Rogers, R. D.; Hunter, W. E.; Atwood, J. L. *Dalton Trans.* **1980**, 1032. (e) de Azevedo, C. G.; Calhorda, M. J.; de C. T. Carrondo, M. A. F.; Dias, A. R.; Duarte, M. T.; Galvão, A. M.; Gamelas, C. A.; Gonçalves, I. S.; da Piedade, F. M.; Romão, C. C. *J. Organomet. Chem.* **1997**, *544*, 257.
- (7) Barlow, S.; Drewitt, M. J.; Dijkstra, T.; Green, J. C.; O'Hare, D.; Whittingham, C.; Wynn, H. H.; Gates, D. P.; Manners, I.; Nelson, J. M.; Pudelski, J. K. *Organometallics* **1998**, *17*, 2113.
- (8) (a) Shapiro, P. J. *Coord. Chem. Rev.* **2002**, *231*, 67. (b) Herbert, D. E.; Mayer, U. F. J.; Manners, I. *Angew. Chem., Int. Ed.* **2007**, *46*, 5060.
- (9) Two examples can be found to the contrary. (1) In the ethene-bridged [2]-ferrocenophane, *ansa*-(vinylene)ferrocene, the *ipso* carbons are located slightly out of the plane formed by the remaining ring carbons with a fold angle of 3.4° . See: (a) Aggarwal, V. K.; Jones, D.; Turner, M. L.; Adams, H. J. *Organomet. Chem.* **1996**, *524*, 263 and (b) Buretea, M. A.; Tilley, T. D. *Organometallics* **1997**, *16*, 1507. (2) In metallocenophanes formed from heterocyclic η^5 -germacyclopentadienyl analogues, buckling of the constituent atoms in the Cp heterocycle reduces the overall strain otherwise expected from introducing a short *ansa* bridge. See: (c) Freeman, W. P.; Dysard, J. M.; Tilley, T. D.; Rheingold, A. L. *Organometallics* **2002**, *21*, 1734.
- (10) For reviews on the ROP of strained [n]ferrocenophanes, see: (a) Kulbaba, K.; Manners, I. *Macromol. Rapid Commun.* **2001**, *22*, 711. (b) Koczagin, I.; Lammertink, R. G. H.; Hempenius, M. A.; Golze, S.; Vancso, G. J. *Adv. Polym. Sci.* **2006**, *200*, 91. (c) Rider, D. A.; Manners, I. *J. Macromol. Sci., Polym. Rev.* **2007**, *47*, 165. (d) Bellas, V.; Rehahn, M. *Angew. Chem., Int. Ed.* **2007**, *46*, 5082. For strained rings based on Cp–M moieties where M is a metal other than Fe, see: (e) Li, C.; Cucullu, M. E.; McIntyre, R. A.; Stevens, E. D.; Nolan, S. P. *Organometallics* **1994**, *13*, 3621. (f) Luo, L.; Zhu, N.; Zhu, N.-J.; Stevens, E. D.; Nolan, S. P. *Organometallics* **1994**, *13*, 669. (g) Herberhold, M. *Angew. Chem., Int. Ed.* **1995**, *34*, 1837. (h) Herberhold, M.; Bärthel, T. *Z. Naturforsch., B: Chem. Sci.* **1995**, *50*, 1692. (i) Vogel, U.; Lough, A. J.; Manners, I. *Angew. Chem., Int. Ed.* **2004**, *43*, 3321. (j) Schachner, J. A.; Tockner, S.; Lund, C. L.; Quail, J. W.; Rehahn, M.; Müller, J. *Organometallics* **2007**, *26*, 4658. For work on strained metallocenophanes containing other π -hydrocarbon ligands, see: (k) Tamm, M.; Kunst, A.; Bannenberg, T.; Herdtweck, E.; Sürsch, P.; Elsevier, C. J.; Ernsting, J. M. *Angew. Chem., Int. Ed.* **2004**, *43*, 5530. (l) Berenbaum, A.; Manners, I. *Dalton Trans.* **2004**, 2057. (m) Elschenbroich, C.; Paganelli, F.; Nowotny, M.; Neumueller, B.; Burghaus, O. *Z. Anorg. Allg. Chem.* **2004**, *630*, 1599. (n) Lund, C. L.; Schachner, J. A.; Quail, J. W.; Müller, J. *Organometallics* **2006**, *25*, 5817. (o) Braunschweig, H.; Kupfer, T.; Radacki, K. *Angew. Chem., Int. Ed.* **2007**, *46*, 1630. (p) Braunschweig, H.; Kupfer, T.; Lutz, M.; Radacki, K. *J. Am. Chem. Soc.* **2007**, *129*, 8893. (q) Lund, C. L.; Schachner, J. A.; Quail, J. W.; Müller, J. *J. Am. Chem. Soc.* **2007**, *129*, 9313. For another novel synthetic variant, see: (r) Sharma, H. K.; Cervantes-Lee, F.; Pannell, K. H. *J. Am. Chem. Soc.* **2004**, *126*, 1326.
- (11) Ni, Y.; Rulkens, R.; Manners, I. *J. Am. Chem. Soc.* **1996**, *118*, 4102.
- (12) Temple, K.; Jäkle, F.; Sheridan, J. B.; Manners, I. *J. Am. Chem. Soc.* **2001**, *123*, 1355.
- (13) Ring-tilted *ansa*-metallocenes are not necessarily strained. Using DFT calculations, Green has shown that the d electron configuration of the metal is what most profoundly influences the geometrical preferences of the *ansa*-[n]metallocenes. See: (a) Green, J. C. *Chem. Soc. Rev.* **1998**, *27*, 263. Unstrained, early transition-metal *ansa*-metallocene complexes are of key importance as molecular catalysts. See: (b) Erker, G. *Macromol. Symp.* **2006**, *236*, 1. (c) Prashar, S.; Antinolo, A.; Otero, A. *Coord. Chem. Rev.* **2006**, *250*, 133. (d) Wang, B. *Coord. Chem. Rev.* **2006**, *250*, 242.
- (14) Berenbaum, A.; Braunschweig, H.; Dirk, R.; Englert, U.; Green, J. C.; Jäkle, F.; Lough, A. J.; Manners, I. *J. Am. Chem. Soc.* **2000**, *122*, 5765.
- (15) (a) Mizuta, T.; Imamura, Y.; Miyoshi, K. *J. Am. Chem. Soc.* **2003**, *125*, 2068. (b) Imamura, Y.; Kubo, K.; Mizuta, T.; Miyoshi, K. *Organometallics* **2006**, *25*, 2301.
- (16) Mizuta, T.; Onishi, M.; Miyoshi, K. *Organometallics* **2000**, *19*, 5005.

[2]metallocenophanes, in which we demonstrate that either reversible or irreversible haptotropic rearrangements from η^5 - to η^1 -Cp are observed depending on the degree of strain present.

Results

1. Irradiation of the Sila[1]ferrocenophane **1 in the Presence of P Donors.** Our entry point was the moderately strained sila[1]ferrocenophane **1** [$\alpha = 20.8(5)^\circ$],²⁰ a well-studied monomer known to form high molecular weight poly(ferrocenylsilanes) through ROP.²¹ Irradiation of a slight excess of **1** in the presence of 1,2-bis(diphenylphosphino)ethane (dppe) in THF at 5 °C led to a haptotropic shift of a Cp ligand from η^5 to η^1 and coordination of the bidentate phosphine ligand to afford the blood red solid [Fe(dppe){(η^5 -C₅H₄)SiMe₂(η^1 -C₅H₄)}] (**5**) in 90% yield (eq 2). The UV-vis spectroscopic profile of the deeply colored solid is dominated by a high-energy transition at 326 nm ($\epsilon = 3400 \text{ M}^{-1} \text{ cm}^{-1}$) that tails across the visible region of the spectrum with a slight shoulder appearing around 440 nm. In contrast, **1** is a red crystalline solid with a well-defined λ_{max} at 478 nm ($\epsilon = 240 \text{ M}^{-1} \text{ cm}^{-1}$).²²



The $^{31}\text{P}\{^1\text{H}\}$ NMR spectrum of **5** consisted of slightly broadened AB doublets at $\delta = 109.4$ and 108.5 ppm ²³ with the same coupling constant [$^2J(\text{P},\text{P}) = 27.2 \text{ Hz}$] assigned to the diastereotopic phosphorus atoms coordinated to the iron center. The $^{29}\text{Si}\{^1\text{H}\}$ NMR spectrum of **5** consisted of a single broad resonance at $\delta = -8.7 \text{ ppm}$, shifted slightly upfield compared to that of **1** ($\delta = -4.6 \text{ ppm}$).

Figure 3 shows the molecular structure of **5** determined by X-ray diffraction. The Fe center in photoproduct **5** possesses piano–stool geometry. The C(1)–Si(1)–C(7) angle [$99.42(10)^\circ$] is larger than that of **1** [$95.7(4)^\circ$], and the angle β of **5** [$14.0(3)^\circ$], between the C(1)–Si(1) bond and its projection onto the plane formed by cyclopentadienyl carbons C(1)–C(5), has decreased significantly [from $37.0(6)^\circ$ for **1**], consistent with reduced ring strain in **5** compared with **1**.²⁰ The bond lengths for C(6)–C(10) [$1.367(3) \text{ \AA}$] and C(8)–C(9) [$1.343(4) \text{ \AA}$] in the σ -bonded Cp ring are shorter than other bond lengths [average $1.490(3) \text{ \AA}$], indicating that the double bonds are located in these positions in the solid state.

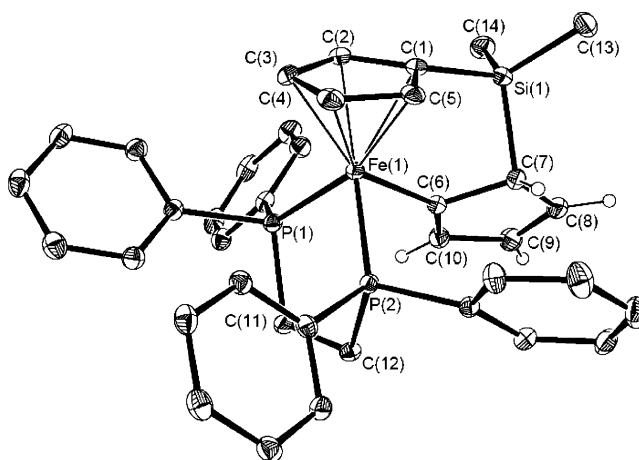


Figure 3. ORTEP of **5** with displacement ellipsoids shown at the 30% probability level. Hydrogen atoms are depicted only for the η^1 -Cp ring. Selected bond distances (\AA) and angles ($^\circ$): Fe(1)–Cp_{centroid} 1.736(2), Fe(1)–P(1) 2.1543(6), Fe(1)–P(2) 2.1544(6), Fe(1)–C(6) 2.015(2), Si(1)–C(1) 1.862(2), Si(1)–C(7) 1.884(2), C(6)–C(7) 1.524(3), C(6)–C(10) 1.367(3), C(7)–C(8) 1.483(3), C(8)–C(9) 1.343(4), C(9)–C(10) 1.464(3), Cp_{centroid}–Fe(1)–C(6) 119.7(9), Cp_{centroid}–Fe(1)–P(1) 129.8(9), Cp_{centroid}–Fe(1)–P(2) 131.5(9), C(1)–Si(1)–C(7) 99.42(10), Fe(1)–C(6)–C(7) 118.01(16), Si(1)–C(7)–C(6) 100.07(14).

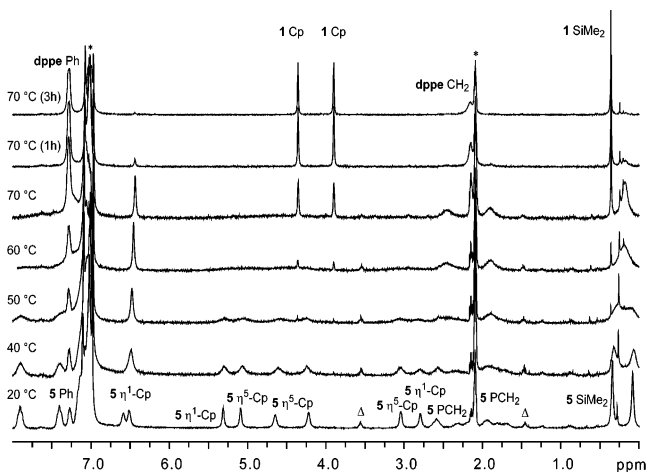


Figure 4. ^1H NMR spectra of **5** in $\text{C}_6\text{D}_5\text{CD}_3$ upon being heated to 70 °C. Asterisks mark peaks from residual toluene (NMR solvent: $\text{C}_6\text{D}_5\text{CD}_3$) and Δ notes residual THF from sample preparation.

In solution, inequivalent proton and carbon signals for the differently coordinated Cp rings were assigned by ^1H – ^1H and ^1H – ^{13}C COSY NMR spectroscopy at -40°C . Interestingly, one ^1H nucleus in each Cp ring was observed at higher field ($\delta = 2.82 \text{ ppm}$ for η^1 -Cp; $\delta = 3.03 \text{ ppm}$ for η^5 -Cp). Upon raising the temperature of the solution to 25 °C, all signals in the ^1H and $^{31}\text{P}\{^1\text{H}\}$ NMR spectra appeared broadened, suggesting fluxional behavior around the Fe center. However, at 25 °C, the two ligands do not interchange quickly on the time scale of the ^1H and ^{13}C NMR spectroscopy experiments, as distinct chemical environments are visible for two Cp rings.

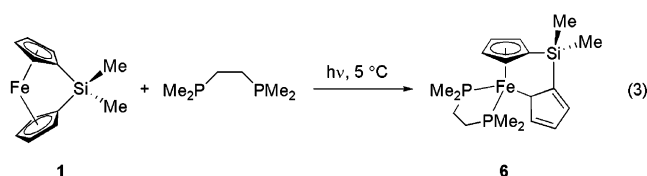
Remarkably, on heating at 70 °C in $\text{C}_6\text{D}_5\text{CD}_3$ for 3 h, photoproduct **5** underwent dissociation of the dppe ligand and quantitative retroconversion into **1** (eq 2). The simplification of the ^{13}C and ^1H NMR spectra (Figure 4) is accompanied by the reappearance of the characteristically upfield-shifted signal assigned to the *ipso* carbon atoms (33.2 ppm) and a downfield shift of the single resonance observed by ^{29}Si NMR spectroscopy (-4.6 ppm), which are retained upon cooling to 20 °C. It appears

- (17) (a) Tanabe, M.; Manners, I. *J. Am. Chem. Soc.* **2004**, *126*, 11434. (b) Tanabe, M.; Vandermeulen, G. W. M.; Chan, W. Y.; Cyr, P. W.; Vanderark, L.; Rider, D. A.; Manners, I. *Nat. Mater.* **2006**, *5*, 467. (c) Chan, W. Y.; Lough, A. J.; Manners, I. *Organometallics* **2007**, *26*, 1217.
- (18) Ieong, N. S.; Chan, W. Y.; Lough, A. J.; Haddow, M. F.; Manners, I. *Chem.–Eur. J.* **2008**, *14*, 1253.
- (19) For a preliminary communication of some of the initial results of this work, see: Tanabe, M.; Bourke, S. C.; Herbert, D. E.; Lough, A. J.; Manners, I. *Angew. Chem., Int. Ed.* **2005**, *44*, 5886.
- (20) Finckh, W.; Tang, B. Z.; Foucher, D. A.; Zamble, D. B.; Ziembinski, R.; Lough, A.; Manners, I. *Organometallics* **1993**, *12*, 823.
- (21) Manners, I. *Chem. Commun.* **1999**, 857.
- (22) Fischer, A. B.; Kinney, J. B.; Staley, R. H.; Wrighton, M. S. *J. Am. Chem. Soc.* **1979**, *101*, 6501.
- (23) These chemical shifts are similar to those of the dppe-coordinated Fe complex [$(\eta^5\text{-Cp})\text{Fe}(\text{dppe})_2(\mu\text{-CH=CHCH=CH})$]. See: Chung, M.-C.; Gu, X.; Etzenhouser, B. A.; Spuches, A. M.; Rye, P. T.; Seetharaman, S. K.; Rose, D. J.; Zubieta, J.; Sponsler, M. B. *Organometallics* **2003**, *22*, 3485.

that **5** is metastable at room temperature and that its formation relies on the photoactivation of **1**. At elevated temperatures, the greater entropy of the species on the left side of eq 2 likely dominates the enthalpic penalty incurred by re-forming the moderately strained **1**.²⁴

Compound **5** slowly dissociates in solution even at room temperature (23 °C). A ³¹P NMR resonance corresponding to dissociated dppe (−12 ppm) appeared (**5**/dppe ≈ 30:1) after a sample of **5** was left in C₆D₆ solution for 1 week. The addition of a donor solvent (THF, 100 equiv) accelerated this process, and a similar ratio was observed between the integrals of the ³¹P signals of **5** and dppe after 1 h. Interestingly, under these conditions, ¹H NMR spectroscopic analysis revealed signals corresponding to **5** and the strained metallocenophane **1** in a ratio of 6:1 after 18 h. The ratio of **5**/dppe, however, was 3:1, which suggested that the dissociation of a molecule of dppe from **5** does not immediately lead to the regeneration of a molecule of **1**, though no solvated intermediates were detected (vide infra). To probe the reactivity of **5** in the presence of excess dppe, ³¹P–³¹P EXSY experiments were conducted for a variety of mixing times (50, 100, and 250 ms) at 22 °C. No cross-peaks were observed between coordinated and free phosphine, demonstrating that no significant exchange is occurring on the NMR time scale at this temperature. The broadening of the phosphorus resonances in the ³¹P NMR spectrum of **5** at room temperature is therefore not likely due to phosphine exchange. The reactivity of **5** in the presence of a better σ-donating phosphine, 1,2-bis(dimethylphosphino)ethane (dmpe), is discussed below.

After similar irradiation of **1** with dmpe, a photoinduced haptotropic shift of a Cp ligand led to the formation of [Fe(dmpe){(η⁵-C₅H₄)SiMe₂(η¹-C₅H₄)}] (**6**), which was isolated as deep purple crystals (eq 3). Mass spectrometry (EI) and elemental analysis supported the identification of the crystalline solid as the adduct **6**. A tailing similar to the case of **5** across the visible region was observed, and shoulders at 350 and 470 nm were detected in the UV–vis spectrum.



Single crystals of **6** were also characterized by X-ray diffraction. The structure of **6** in the solid state (Figure 5) is analogous to that of **5**: the C(1)–Si(1)–C(18) angle [100.9(4)°] is larger than that in **1** [95.7(4)°] and the angle β (16.5°) has again decreased significantly. Notably, at 2.249(9) Å, the Fe–C(14) distance between the metal center and the σ-bound Cp ring is significantly longer (0.23 Å) than the Fe–C(η¹-Cp) bond distance in **5** [2.015(2) Å].

The molecular structure of **6** in solution is more ambiguous than that for **5**. At 20 °C, the ³¹P{¹H} NMR spectrum of an analytically pure sample of **6** showed a single broad signal centered at δ = 78 ppm. At 0 °C, two broad signals appeared downfield from the single resonance, and at −20 °C, these

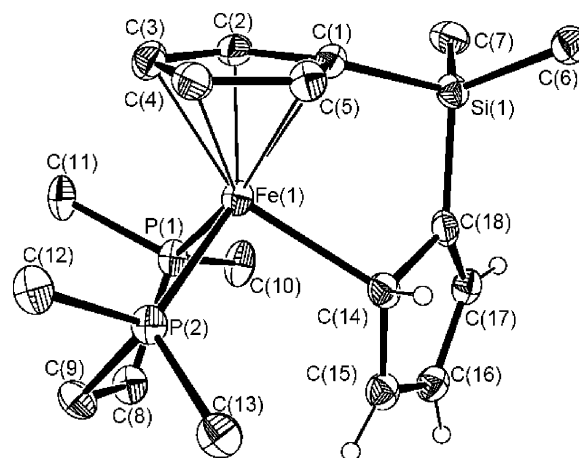


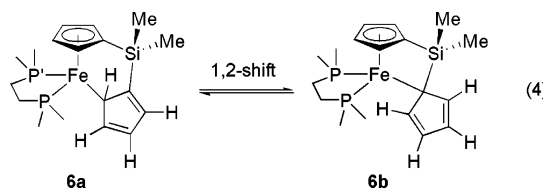
Figure 5. ORTEP of **6** with displacement ellipsoids shown at the 30% probability level. Hydrogen atoms are omitted except for the η¹-Cp ring. Selected bond distances (Å) and angles (°): Fe(1)–Cp_{centroid} 1.717(10), Fe(1)–P(1) 2.176(3), Fe(1)–P(2) 2.179(3), Fe(1)–C(14) 2.249(9), Si(1)–C(1) 1.867(9), Si(1)–C(18) 1.833(10), C(18)–C(17) 1.371(13), C(17)–C(16) 1.429(14), C(16)–C(15) 1.375(14), C(15)–C(14) 1.453(14), C(14)–C(18), 1.468(13), Cp_{centroid}–Fe(1)–C(14) 120.3(4), Cp_{centroid}–Fe(1)–P(1) 125.1(3), Cp_{centroid}–Fe(1)–P(2) 127.3(3), C(1)–Si(1)–C(18) 100.9(4), Fe(1)–C(14)–C(18) 105.1(6), Si(1)–C(18)–C(14) 120.2(7).

Table 1. Effect of Temperature on the Proposed Equilibrium between **6a** and **6b**

T (K)	integral ratio 6b / 6a ^a	ΔG _{eq} (kJ/mol) ^b
273	5.4:1	−3.8
253	6.3:1	−3.9
233	8.1:1	−4.1
213	11.3:1	−4.3
193	16.5:1	−4.5

^a Determined from ³¹P{¹H} NMR spectroscopy. ^b Calculated from ΔG = −RT ln K_{eq}.

sharpened into two doublets (δ = 88.2 and 85.4 ppm, ²J(P,P) = 38 Hz) while the broad resonance (δ = 78 ppm) narrowed to a singlet (δ = 80 ppm, −80 °C). These two independent spin systems could arise from two possible structural isomers: one with diastereotopic phosphorus environments (e.g., **6a**) and one without (e.g., **6b**). The apparent equilibrium between the two isomers slightly favors the symmetric isomer, increasingly so at lower temperatures (eq 4, Table 1).



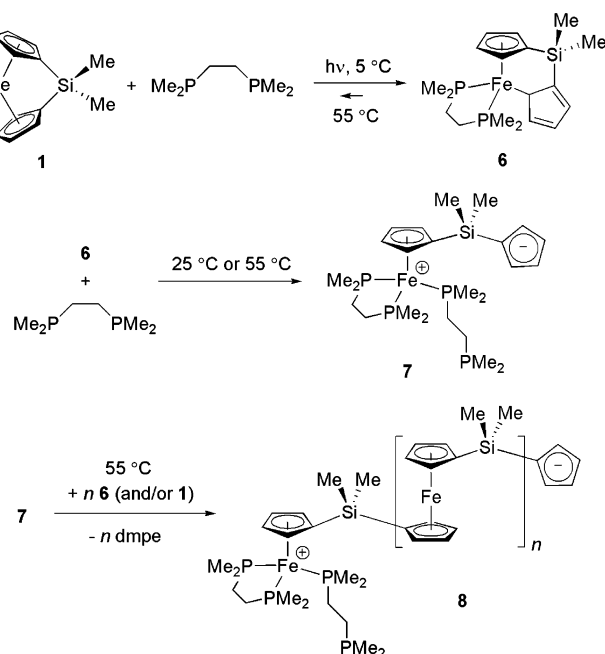
Interestingly, unlike the case of **5**, heating a C₆D₆ solution of **6** at 55 °C for 4 h failed to regenerate the sila[1]-ferrocenophane **1** as an identifiable product. The ¹H NMR spectra of a C₆D₆ solution of **6** did not indicate any retroconversion when monitored in 10° increments up to 75 °C over 1 h. However, a small proportion of uncoordinated dmpe [δ(³¹P{¹H}) = −48 ppm; ratio of **6**/dmpe ≈ 200:1] was observed on reaching 55 °C. After further heating over an additional 12 h, 100% conversion of the ³¹P NMR signal for **6** [δ(³¹P{¹H}) = 77.6 ppm] into a new AMX spin system [δ(³¹P{¹H}) = 75.2 (doublet, ²J(P,P) = 57 Hz), 34.9 (doublet of triplets, ²J(P,P) = 57 Hz, ³J(P,P) = 22 Hz), −47.3 ppm (doublet, ³J(P,P) = 22 Hz)] and free dmpe (−48 ppm) was observed. ¹H NMR

(24) The AB doublets in the ³¹P NMR spectra of **5** appear to collapse asymmetrically approaching 70 °C, possibly because of the initial release of a single end of the bis(phosphine) ligand. See Supporting Information.

Table 2. Thermal Ring-Opening Polymerization^a of **6**

[6] (M)	<i>T</i> (°C) ^a	yield (%) ^b	<i>M_w</i>	PDI
0.01	60	<5		
0.10	60	29	3410	1.35
0.24	55	37	5230	1.37
0.51	55	40	5070	1.35
0.98	55	42	4104	1.35

^a Reactions were all performed in THF and heated for 12 h. No unreacted **6** was observed after this time. ^b Isolated yield of polymer after multiple precipitations (2–3) into MeOH.

Scheme 1. Proposed Mechanism for the Thermal Polymerization of **6**

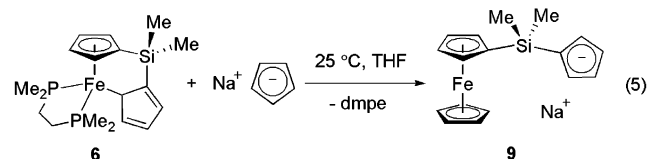
spectroscopic analysis suggested that the thermal treatment of **6** over 12 h had formed poly(ferrocenyldimethylsilane) **8** with an end group consisting of one bidentate and one monodentate dmpe ligand (seen in the AMX spin system observed by ³¹P-{¹H} NMR spectroscopy) and free dmpe. Repeat trials at various initial molar concentrations of **6** produced identical results, and the molecular weights of the polymers were determined by gel permeation chromatography (GPC, Table 2).

A plausible mechanism for the thermal ring-opening polymerization of **6**, outlined in Scheme 1, begins with thermal dissociation of dmpe from a small fraction of **6**, which then can substitute the η^1 -Cp ring from a second equivalent to form the zwitterionic species **7**. The latter could then function as an ROP initiator, assuming the rate of propagation of the growing polymer chain exceeds the rate of addition of a second equivalent of dmpe to **6**. Thus, the pendant Cp anion of **7** could initiate the thermal ring-opening polymerization of the remaining ring-slipped species **6** with extrusion of dmpe, or alternatively via the ROP of **1**. As noted previously, Miyoshi et al. have reported polymerization of phosphite adducts of phosphat[1]-ferrocenophanes (e.g., **4**) in refluxing THF¹⁶ and Cp anions have been shown to induce the ROP of **1** upon irradiation at 5–25 °C.¹⁷

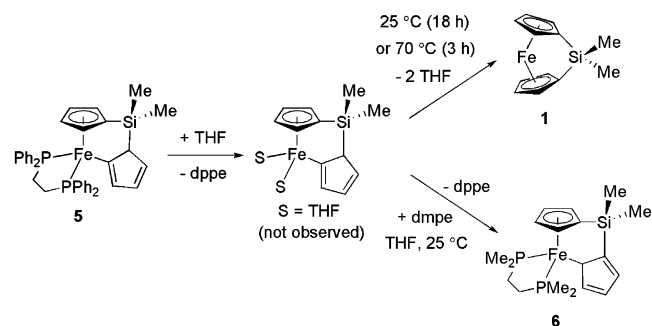
To examine the likelihood for the formation of the proposed initiator (**7**), two additional equivalents of dmpe were added to a solution of **6** at 25 °C. After 2 days, the zwitterionic **7** was

tentatively assigned in situ by the appearance of an AMX spin system in ³¹P-{¹H} NMR spectra identical to that observed following the initial heating of **6** for an extended period (12 h). The proposed structure of **7** was supported by ¹H NMR spectroscopic characterization and electrospray mass spectrometry (ESI-MS) analysis of a freshly prepared sample (Experimental Section in Supporting Information); however, repeated attempts at the further isolation of **7** in the solid state led only to insoluble decomposition products.

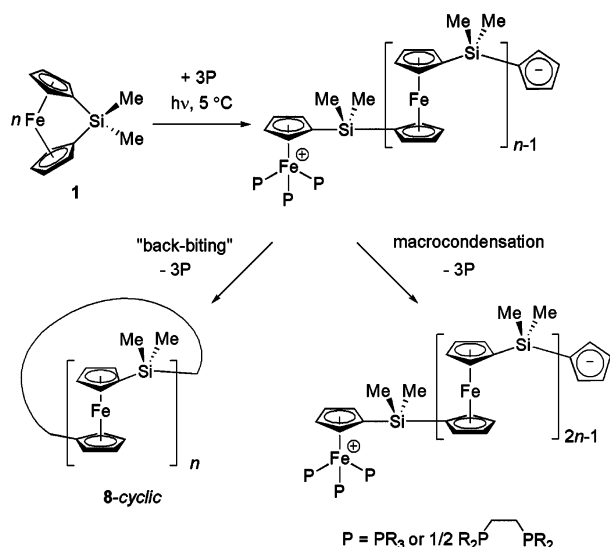
To elaborate on the proposed propagation step in the thermal polymerization of **6**, we also investigated the reactivity of this species toward Cp anions. Na[C₅H₅] and **6** were stirred in THF in the absence of light. After 1 h at 25 °C, dmpe was substituted from **6** (observed by ³¹P-{¹H} NMR spectroscopy) and the color of the solution changed from black to bright yellow (eq 5). The previously reported ring-opened species **9** was subsequently identified by ¹H NMR spectroscopy.^{17a} While **1** is unreactive toward Cp anions at 25 °C in THF in the absence of light,^{17a} [C₅H₅][−] was found to initiate the ROP of **1** in polar solvents (THF, pyridine) at elevated temperatures (55 °C). Therefore, if the process to generate the pendant Cp[−] propagating anion begins with the thermal dissociation of dmpe from a small amount of **6** re-forming **1**, the regenerated metallocenophane could be consumed as additional monomer by a propagating polymer chain at 55 °C.



While **5** was found to be unreactive in the presence of excess dppe, in the presence of a better σ -donor phosphine (dmpe) the ring-slipped compound **5** was completely consumed over 2 h. The addition of dmpe in THF, however, did not lead to substitution of the η^1 -Cp ring at the Fe center, rather quantitative phosphine exchange produced **6** and uncoordinated dppe (Scheme 2). As the coordinated dppe ligand in **5** was observed to dissociate in the presence of THF (vide supra), the addition of dmpe likely intercepts a solvated transient (η^5 , η^1) ferrocenophane (which may possess a monodentate dppe ligand) before it can retroconvert to **1**.

Scheme 2. Possible Mechanism for Phosphine Exchange To Produce **6** from **5**

Irradiation of a THF solution of **1** and 1,2-bis(di-*tert*-butylphosphino)ethane (d**t**bpe) produced a yellow-orange reaction mixture. No evidence of coordination of 1 equiv of d**t**bpe to trap a mixed hapticity metallocenophane was observed.

Scheme 3. Photocontrolled Polymerization Behavior of **1** with Phosphine Initiators

Instead, as suggested by the color of the reaction mixture, ROP of **1** to form polyferrocenylsilane $[Fe(\eta^5-C_5H_4)_2SiMe_2]_n$ was confirmed by 1H NMR spectroscopy. GPC analysis showed the product possessed a bimodal molecular weight distribution ($M_n = 4450$, PDI = 1.1 and $M_n = 24\,880$, PDI = 1.6). However, no evidence of incorporation of d'bpe end groups into the polymer chain could be detected by 1H or ^{31}P NMR spectroscopy despite the low molecular weights.^{25a} MALDI-TOF MS analysis of the low molecular weight fraction of the polymer suggested that back-biting by the propagating Cp[−] anion to replace the bulky P donor ligand had occurred, resulting in a mass spectrum corresponding to exact integer values of the monomer **1** consistent with the cyclic structure of **8-cyclic** (Scheme 3, Figure 6).^{25b} The higher molecular weight fraction of the bimodal distribution may have resulted from macrocondensation of two or more polymer chains. However, the end group structure of the higher molecular weight fraction could not be confirmed as this fraction did not ionize under the experimental conditions employed.

Monodentate phosphines (PR_3 ; R = Me, Ph) were found to promote photolytic ROP of **1** at 5–25 °C regardless of reaction stoichiometry (Scheme 3, Table 3). Irradiation of **1** with excess PMe_3 in C_6D_6 at room temperature for 5 h afforded the ring-opened polymer $[Fe(\eta^5-C_5H_4)_2SiMe_2]_n$ with 100% conversion and in 35% isolated yield ($M_n = 1.3 \times 10^4$, PDI = 1.4),²⁶ supporting the assertion that the rate of polymer propagation is faster than the rate of formation of ring-slipped adducts.

Surprisingly, the photocontrolled polymerization induced by PPh_3 even occurred in the presence of Me_3SiCl (Table 3, runs 5–7), which has been previously used as a reagent for anionic chain termination. A few drops of a protic solvent (e.g., water) are typically added to polymer solutions to quench the “living” chain end produced by anionic ROP of $[n]$ metallocenophanes.¹¹

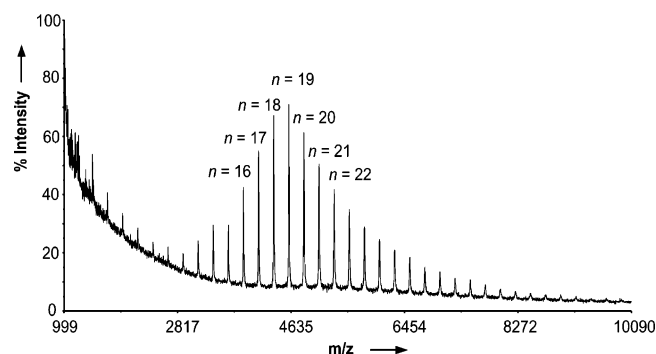
Table 3. Photolytic ROP of **1** Initiated by P Donors

run	initiator (M/I) ^a	solvent	conditions	M_n^b	M_w^b	PDI	MALDI ^c
1	PMe_3 (1:2)	C_6D_6	5 h	25 °C	13000	18850	1.4
2	PMe_3 (1:3)	THF	5 h	5 °C	2450	3140	1.3
3	PPh_3 (1:1)	THF	3 h	5 °C	27420	146470	5.3
4	PPh_3 (1:5)	THF	3 h	5 °C	24510	66650	2.7
5	PPh_3 (1:3)	THF ^d	2 h	5 °C	20370	46850	2.3
6	PPh_3 (1:3)	Me_3SiCl	5 h	5 °C	5590	7120	1.3
7	PPh_3 (1:3)	Me_3SiCl	3 h	5 °C	4950	7790	1.6
8	d'bpe (1:1)	THF	3 h	5 °C	4450	4980	1.1
					24880	39280	1.6

^a Ratio of monomer to initiator. ^b Determined by conventional GPC.

^c Highest MW peak observed in MALDI-TOF MS (linear mode) with degree of polymerization (DP_n) in the adjacent parentheses. Under our experimental conditions, only lower molecular weight fractions (<10 000 Da) ionized.

^d Solvent: THF + 1 equiv of Me_3SiCl .

**Figure 6.** MALDI-TOF MS (linear (+) mode with dithranol as matrix) of d'bpe-initiated **8-cyclic** (Table 3, run 8). The most intense peak (4600 m/z) corresponds to a chain length of 19 repeat units.

In place of protic quenching, chloro(triorgano)silanes have been used to assist in the detection of polymer end groups.²⁵ The formation of polymer in neat Me_3SiCl (Table 3, runs 6 and 7) indicates that chain propagation is faster than the substitution reaction of the propagating Cp^- anion with the chlorosilane.²⁷

While monomer conversions were typically high (~80%), isolated polymer yields were low (20–40%). Shorter oligomers, which did not precipitate during the polymer workup, and ring-opened monomer were identified as the other major products by 1H and ^{31}P NMR spectroscopy. For example, while a broad singlet in the $^{31}P\{^1H\}$ NMR spectrum (at 25 ppm) suggested coordinated P donors for run 2, no end groups were observed for any of the isolated polymers by multinuclear NMR spectroscopy, consistent with the cyclic structures suggested by MALDI-TOF analysis (Scheme 3, Table 3).

2. Irradiation of the [2]Ferrocenophane **10 in the Presence of P Donors.** To explore the generality of the surprising reversible haptotropic shifts and other unusual [1]ferrocenophane reactivity of **1** described above, we investigated the analogous chemistry of the ethane-bridged [2]ferrocenophane **10** [$\alpha = 21.6(4)^\circ$],²⁸ which has a tilt angle similar to that of **1**, suggesting a similar degree of ring strain. No reaction was observed upon irradiation of **10** in the presence of dppe in THF. However, another ring-slipped Fe complex, $[Fe(dmpe)\{(\eta^5-C_5H_4)(CH_2)_2-$

(25) (a) Multinuclear NMR spectroscopy has been used to identify Me_3Si end groups in oligoferrocenylsilanes with molar masses up to 2000 Da. See: ref 11 and Rulkens, R.; Lough, A. J.; Manners, I.; Lovelace, S. R.; Grant, C.; Geiger, W. E. *J. Am. Chem. Soc.* **1996**, *118*, 12683. (b) For a recent report on the production and characterization of metallomacrocycles and cyclic polymers, see: Chan, W. Y.; Lough, A. J.; Manners, I. *Angew. Chem., Int. Ed.* **2007**, *46*, 9069.

(26) Foucher, D. A.; Tang, B. Z.; Manners, I. *J. Am. Chem. Soc.* **1992**, *114*, 6246.

(27) The lower molecular weights obtained from P donor promoted ROP in neat Me_3SiCl are likely due to a solvent polarity effect (compare runs 4–7, Table 3).

(28) (a) Lentzner, H. L.; Watts, W. E. *Tetrahedron* **1971**, *27*, 4343. (b) Nelson, J. M.; Rengel, H.; Manners, I. *J. Am. Chem. Soc.* **1993**, *115*, 7035. (c) Nelson, J. M.; Nguyen, P.; Petersen, R.; Rengel, H.; Macdonald, P. M.; Lough, A. J.; Manners, I.; Raju, N. P.; Greedan, J. E.; Barlow, S.; O'Hare, D. *Chem.-Eur. J.* **1997**, *3*, 573.

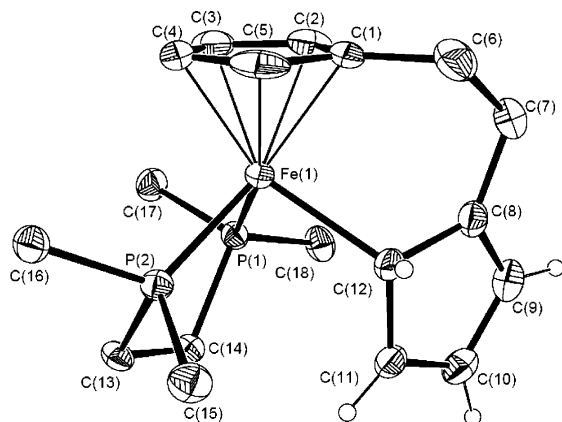
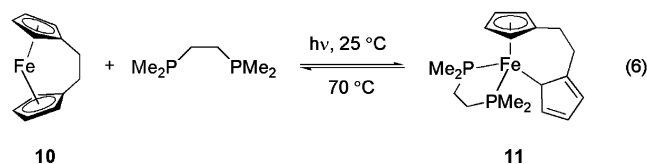


Figure 7. ORTEP of **11** with displacement ellipsoids shown at the 30% probability level. Hydrogen atoms are depicted only for the η^1 -Cp ring. Selected bond distances (Å) and angles ($^\circ$): Fe(1)–Cp_{centroid} 1.717(5), Fe(1)–P(1) 2.167(2), Fe(1)–P(2) 2.178(1), Fe(1)–C(12) 2.201(5), C(1)–C(6) 1.491(8), C(6)–C(7) 1.516(9), C(7)–C(8) 1.512(7), C(8)–C(9) 1.352(8), C(8)–C(12) 1.476(7), C(9)–C(10) 1.428(8), C(10)–C(11) 1.350(8), C(11)–C(12) 1.465(7), Cp_{centroid}–Fe(1)–C(12) 120.1(2), Cp_{centroid}–Fe(1)–P(1) 125.1(2), Cp_{centroid}–Fe(1)–P(2) 128.0(2), C(1)–C(6)–C(7) 111.6(5), C(6)–C(7)–C(8) 113.5(5), C(7)–C(8)–C(12) 124.6(5), Fe(1)–C(12)–C(8) 110.6(3).

(η^1 -C₅H₄)] (**11**), was obtained from irradiation of **10** in the presence of dmpe in THF at 25 $^\circ$ C (eq 6). Recrystallization of the crude product from toluene/hexane at –55 $^\circ$ C afforded **11** as dark red crystals in 83% yield.



Complex **11** was fully characterized by one- and two-dimensional NMR spectroscopic methods at low temperature, and the molecular structure was determined by X-ray diffraction (Figure 7). The piano–stool Fe center is again capped by an η^5 -Cp ligand, while the chelating dmpe ligand and σ -bound Cp ring are arranged as a tripod base. The C(1)–C(6) bond was found to lie almost in the plane of the η^5 -Cp ligand [β = 1.9–(3) $^\circ$], indicating that the structure contains no significant ring strain. The two double bonds in the η^1 -Cp ring were located at C(8)–C(9) [1.352(8) Å] and C(10)–C(11) [1.350(8) Å], supported by the conformation about C(12), which is unsuited to an sp² carbon center.

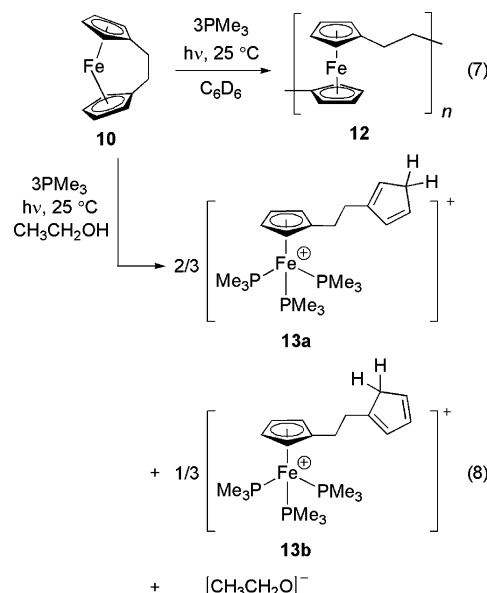
Variable-temperature $^{31}\text{P}\{^1\text{H}\}$ NMR spectra of **11** exhibited two doublets at δ = 81.0 and 78.9 ppm ($^2J(\text{P,P})$ = 39 Hz) at –40 $^\circ$ C that coalesced into a single signal at 79.0 ppm upon warming to 20 $^\circ$ C. At –60 $^\circ$ C, the ^1H NMR spectrum contained eight signals attributed to the two inequivalent Cp rings in the range δ = 1.70–6.64 ppm. When the temperature was raised to –20 $^\circ$ C, all signals broadened and coalescence was observed around 0 $^\circ$ C (Supporting Information).

The fluxional behavior of σ -bound Cp rings such as those in [Fe(η^1 -Cp)(η^5 -Cp)(CO)₂] has been well studied.²⁹ The η^1 -Cp ligand of this species is involved in a fluxional process that consists of successive 1,2-shifts, observable on the NMR time

scale, while the η^5 -Cp ring signals display no coalescence because of more rapid ring rotation. The dynamic nature of the NMR spectrum of **11** suggests fluxional behavior, which may involve fast successive 1,2-shifts of the η^1 -Cp ring. Slow coordination mode exchange between the two Cp ligands can be ruled out by virtue of the four inequivalent resonances, two arising from inequivalent quaternary carbon nuclei and two attributed to the distinct bridging ethylene carbons, observed at room temperature by ^{13}C NMR spectroscopy. As with **5**, heating **11** in C₆D₅CD₃ for 3 h at 70 $^\circ$ C led to a quantitative reverse haptotropic rearrangement with dissociation of the dmpe ligand and the regeneration of moderately strained **10** (eq 6).

Also analogous to the behavior of the [1]ferrocenophane **1**, monodentate P donors promoted ROP of **10**. Irradiation of a solution of **10** with 3 equiv of PMe₃ for 3 h in C₆D₆ led to the yellow insoluble polymer **12** in 66% isolated yield (eq 7).^{28b,c} To directly observe the role of the P donor in promoting ROP, we reinvestigated this reaction with the aim of trapping the zwitterionic intermediate generated in the initiation step. However, as the quenching reaction of pendant Cp[–] anions generated from ring-opened metallocenophanes with chloro-(triorgano)silane capping agents was found to be inefficient for **1** (section 1, Table 3), we sought a more reactive quenching source and employed a protic solvent (ethanol).³⁰

Irradiation of **10** and 3 equiv of trimethylphosphine in ethanol (eq 8) produced a yellow reaction mixture that showed a new $^{31}\text{P}\{^1\text{H}\}$ resonance at 25 ppm attributed to a ring-opened product. The product **13**[OCH₂CH₃] was isolated in 80% yield as a mustard-yellow powder that was further analyzed by ESI-MS. Exchanging ethoxide for a larger tetraphenylborate anion with Na[BPh₄] allowed for the isolation of an air-stable yellow powder. In solution, two structural isomers that differ only in the position of the fifth proton on the pendant cyclopentadienyl ring (cf. **6**, eq 4) were observed in a 2:1 ratio (**13a**/**13b**) by ^1H NMR spectroscopy. Dark orange single crystals of the minor isomer, **13b**[BPh₄], suitable for X-ray diffraction were grown from diethylether-rich solutions of THF and diethylether.



The solid-state structure of **13b**[BPh₄] (Figure 8) contains a pendant, protonated cyclopentadienyl group directed away from

(29) (a) Bennett, M. J., Jr.; Cotton, F. A.; Davison, A.; Faller, J. W.; Lippard, S. J.; Morehouse, S. M. *J. Am. Chem. Soc.* **1966**, *88*, 4371. (b) Cotton, F. A. *Acc. Chem. Res.* **1968**, *1*, 257. (c) Wright, M. E.; Nelson, G. O.; Glass, R. S. *Organometallics* **1985**, *4*, 245.

(30) Protic solvents react with sila[1]ferrocenophanes via ring-opening protonolysis at the C_{ipso}–Si bond, and thus this reaction could not be explored for species **1**.

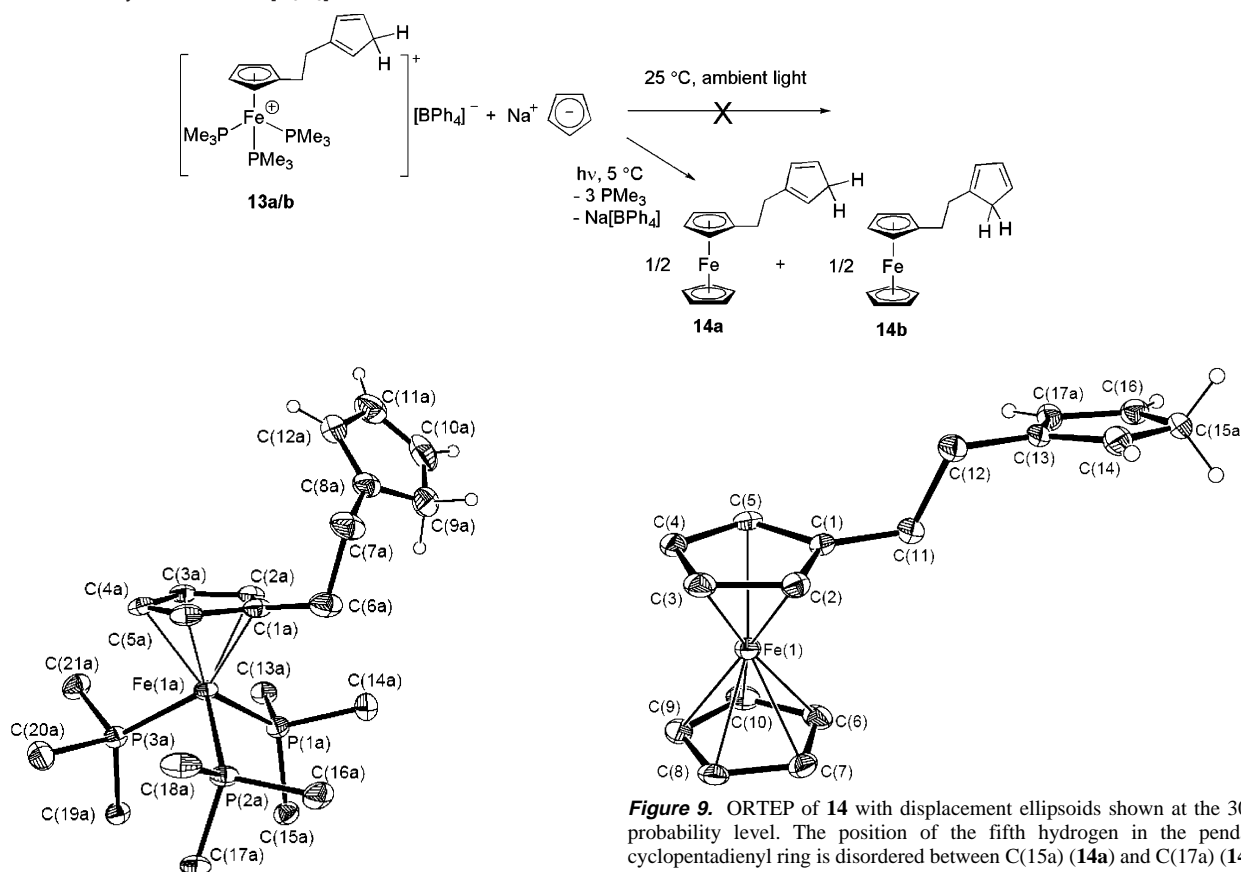
Scheme 4. Reactivity of **13** with Na[C₅H₅]

Figure 8. ORTEP of the cation of **13b** [BPh₄][−] with displacement ellipsoids shown at the 30% probability level. The anion and all hydrogens except for the pendant cyclopentadienyl ring are omitted for clarity. Selected bond distances (Å) and angles (°): Fe(1a)–P(1a) 2.202(1), Fe(1a)–P(2a) 2.215(1), Fe(1a)–P(3a) 2.222(1), Fe(1a)–Cp_{centroid} 1.734(5), C(1a)–C(6a) 1.518(7), C(6a)–C(7a) 1.551(8), C(7a)–C(8a) 1.497(8), C(8a)–C(12a) 1.342(8), C(8a)–C(9a) 1.479(9), C(9a)–C(10a) 1.413(10), C(10a)–C(11a) 1.365(10), C(11a)–C(12a) 1.494(9), Cp_{centroid}–Fe(1a)–P(1a) 120.2(2), Cp_{centroid}–Fe(1a)–P(2a) 123.7(2), Cp_{centroid}–Fe(1a)–P(3a) 119.1(2), Cp_{centroid}–C(1a)–C(6a) 6.7(5), C(1a)–C(6a)–C(7a) 112.3(4), C(6a)–C(7a)–C(8a) 113.3(5), C(8a)–C(9a)–C(10a) 105.8(5), C(9a)–C(10a)–C(11a) 110.7(6), C(10a)–C(11a)–C(12a) 106.6(6), C(11a)–C(12a)–C(8a) 108.4(6), C(12a)–C(8a)–C(9a) 108.6(6).

the piano–stool PMe₃-substituted iron center. The bond angles in cation **13b** are not significantly altered from values typical for similar organometallic complexes. For one of the two cations located in the unit cell, the bond distances C(8)–C(12) [1.342(8) Å] and C(11)–C(10) [1.365(10) Å] indicate that the double bonds of the terminal Cp ring are located between these carbons and the fifth hydrogen is on C(9). However, for the second cation, the C(11)–C(10) distance is slightly longer [1.438(14) Å] than the C(9)–C(10) separation. Additionally, the small internal ring angles about C(11) [106.6(6), 101.7(8)°], short distances between C(9) and C(10) [1.413(10), 1.401(12) Å] relative to sp³–sp² distances in cyclopentadiene (computational 1.499 Å; microwave 1.505 Å),³¹ and large displacement ellipsoids for some of the ring atoms suggest structural disorder with a small proportion of C(11) sp³ hybridized (**13a**).

Figure 9. ORTEP of **14** with displacement ellipsoids shown at the 30% probability level. The position of the fifth hydrogen in the pendant cyclopentadienyl ring is disordered between C(15a) (**14a**) and C(17a) (**14b**) with equal occupancy. Only one isomer (**14a**) is shown for clarity, with hydrogens omitted except for the cyclopentadienyl ring. Selected bond distances (Å) and angles (°): C(13)–C(14) 1.352(6), C(14)–C(15a) 1.465(7), C(15a)–C(16) 1.382(6), C(16)–C(17a) 1.430(6), C(13)–C(17a) 1.430(6), C(13)–C(14)–C(15a) 109.2(4), C(14)–C(15a)–C(16) 107.3, C(15a)–C(16)–C(17a) 109.0(4), C(16)–C(17a)–C(13) 106.5(4), C(14)–C(13)–C(17a) 108.1(4).

Studies of the reactivity of **13** toward Cp anions allowed us to investigate the “back-biting” step proposed to occur to produce cyclic poly(ferrocenyldimethylsilane) **8-cyclic** from the photocontrolled, P donor promoted ROP of **1** (Scheme 3). No change in the ³¹P{¹H} NMR spectrum of **13**[BPh₄][−] was observed after being stirred in THF with more than 1.5 equiv of Na[C₅H₅] for 1.5 h under ambient light. However, mimicking the conditions of the P donor promoted polymerizations quantitatively liberated PMe₃ after 1.3 h of irradiation at 5 °C (Scheme 4). Thus, remarkably, the cyclization or macrocondensation side reactions involving phosphine substitution (Scheme 3) therefore likely operate under the photocontrolled ROP conditions examined. The molecular structure of **14** is shown in Figure 9.

3. Reactions of [2]Ruthenocenophanes **15 and **16** with P Donors.** As the reactivity of [*n*]ferrocenophanes toward P donors varies subtly with the electronic and steric properties of the incoming Lewis base, we decided to investigate the effect of increased ring strain in [*n*]metallocenophanes by exploring the analogous reactivity of ethane-bridged [2]ruthenocenophanes **15**³² and **16**,³³ which possess larger tilt angles of 29.6(5)° (**15**) and 31.1° (**16**) by virtue of the larger covalent radius of Ru relative to that of Fe.³⁴ When reacted with excess dmpe without irradiation, the new complexes [Ru(dmpe){(η⁵-C₅H₄)(CR₂)₂(η¹-

(31) (a) Damiani, D.; Ferretti, L.; Gallinella, E. *Chem. Phys. Lett.* **1976**, 37, 265. (b) Jiao, H.; von Ragué Schleyer, P. *Faraday Trans.* **1994**, 90, 1559.

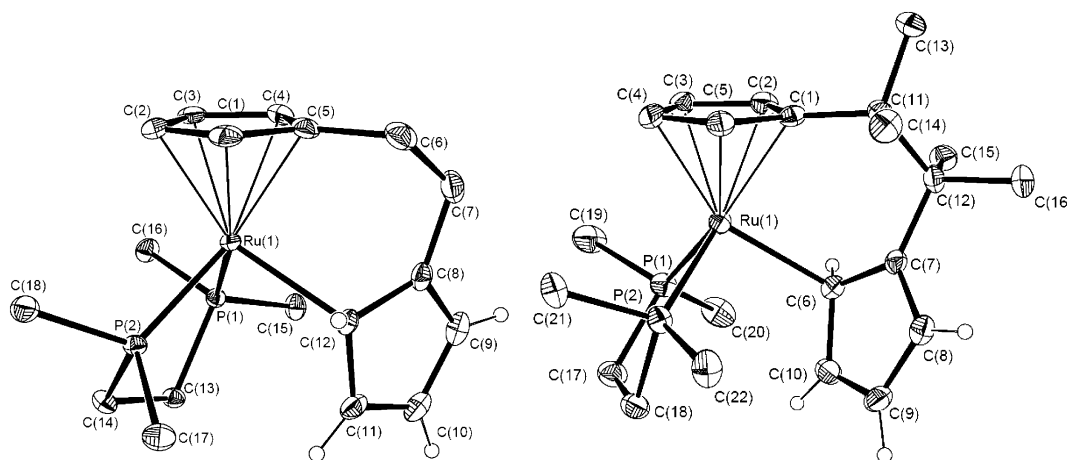
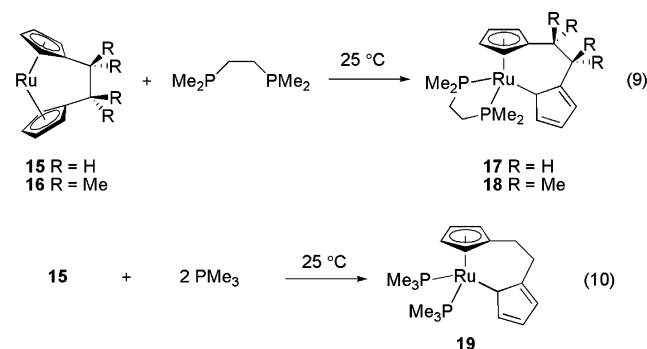


Figure 10. Molecular structures of **17** (left) and **18** (right) (one of two molecules in the asymmetric unit) with displacement ellipsoids shown at the 30% probability level. Hydrogen atoms are depicted only for the η^1 -Cp rings. Selected bond distances (Å) and angles (°) for **17**: Ru(1)–Cp_{centroid} 1.870(3), Ru(1)–P(1) 2.2501(7), Ru(1)–P(2) 2.2544(8), Ru(1)–C(12) 2.266(3), C(5)–C(6) 1.494(5), C(6)–C(7) 1.520(5), C(7)–C(8) 1.507(5), C(8)–C(9) 1.363(5), C(8)–C(12) 1.482(5), C(9)–C(10) 1.430(5), C(10)–C(11) 1.351(5), C(11)–C(12) 1.463(5), Cp_{centroid}–Ru(1)–C(12) 117.6(1), Cp_{centroid}–Ru(1)–P(1) 128.5(9), Cp_{centroid}–Ru(1)–P(2) 128.7(9), C(5)–C(6)–C(7) 112.7(3), C(6)–C(7)–C(8) 114.3(3), C(7)–C(8)–C(12) 126.2(3), Ru(1)–C(12)–C(8) 107.8(2). Selected bond distances (Å) and angles (°) for **18**: Ru(1)–Cp_{centroid} 1.878(5), Ru(1)–P(1) 2.2557(13), Ru(1)–P(2) 2.2513(13), Ru(1)–C(6) 2.276(5), C(1)–C(11) 1.517(6), C(11)–C(12) 1.595(7), C(12)–C(7) 1.523(6), C(7)–C(8) 1.374(6), C(6)–C(7) 1.471(6), C(8)–C(9) 1.427(7), C(6)–C(10) 1.449(6), C(10)–C(9) 1.352(7), Cp_{centroid}–Ru(1)–C(6) 120.0(2), Cp_{centroid}–Ru(1)–P(1) 130.5(1), Cp_{centroid}–Ru(1)–P(2) 125.1(1), C(1)–C(11)–C(12) 113.0(4), C(11)–C(12)–C(7) 111.0(4), C(12)–C(7)–C(6) 125.5(4), Ru(1)–C(6)–C(7) 107.7(3).

C₅H₄}] (**17** R = H, **18** R = Me) formed in quantitative yields (eq 9).



The solid-state structures of **17** and **18** were investigated by single-crystal X-ray diffraction. The molecular structures (Figure 10) and the η^1 -Cp ring geometry are comparable to that observed for complex **11**. The Cp_{centroid}–Ru distances (1.87 Å, average **17** and **18**) are longer than the Cp_{centroid}–Fe distance in **11** (1.72 Å) because of the larger size of the ruthenium atom.

As expected from the reaction in the absence of UV irradiation, the ring-slipped Ru complexes **17** and **18** are more thermodynamically stable compounds compared to **15** and **16**, relative to the analogous Fe systems, likely because of the high

ring strain energy of ruthenocenophanes **15** and **16**. In fact, monitoring a sample of **17** in C₆D₅CD₃ heated extensively at 110 °C by ¹H NMR spectroscopy did not reveal detectable retroconversion to **15**.

Surprisingly, irreversible formation of a ring-slipped η^1 -Cp complex [Ru(PMe₃)₂{(η^5 -C₅H₄)(CH₂)₂(η^1 -C₅H₄)}] (**19**) also occurred upon mixing **15** with an excess of the monodentate phosphine PMe₃ (eq 10, Figure 11). No ROP of the highly strained [2]ruthenocenophanes was observed in the presence of excess PMe₃ at 55 °C, a consequence of more stable metal–(η^1 -Cp) bonding (vide infra). Neither were the PMe₃ ligands displaced by chelating P donors when **19** was heated to 55 °C in the presence of dmpe or d'bpe (2.5 h).

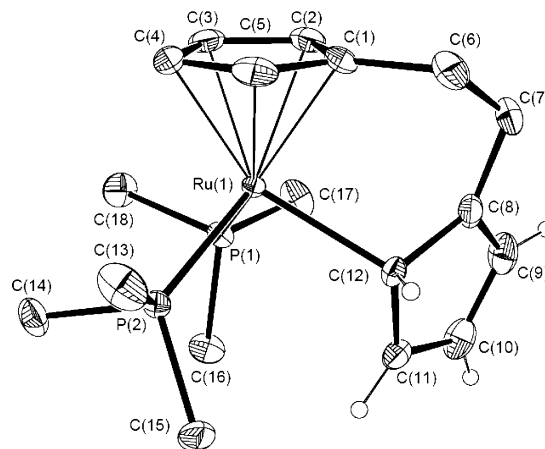


Figure 11. ORTEP of **19** with displacement ellipsoids shown at the 30% probability level. Hydrogen atoms are depicted only for the η^1 -Cp ring. Selected bond distances (Å) and angles (°): Ru(1)–Cp_{centroid} 1.863(3), Ru(1)–P(1) 2.2710(6), Ru(1)–P(2) 2.2719(6), Ru(1)–C(12) 2.275(2), C(1)–C(6) 1.505(4), C(6)–C(7) 1.496(5), C(7)–C(8) 1.508(4), C(8)–C(12) 1.474(3), C(8)–C(9) 1.355(4), C(8)–C(12) 1.474(3), C(9)–C(10) 1.425(5), C(10)–C(11) 1.360(4), C(11)–C(12) 1.464(4), Cp_{centroid}–Ru(1)–C(12) 117.3(9), Cp_{centroid}–Ru(1)–P(1) 124.4(9), Cp_{centroid}–Ru(1)–P(2) 123.9(9), C(1)–C(6)–C(7) 112.8(3), C(6)–C(7)–C(8) 114.4(3), C(7)–C(8)–C(12) 126.0(3), Ru(1)–C(12)–C(8) 108.23(16).

- (32) Nelson, J. M.; Lough, A. J.; Manners, I. *Angew. Chem., Int. Ed.* **1994**, *33*, 989.
- (33) Reactant **16** was prepared via an alternative synthesis to that previously reported by Herberhold et al. in ref 10h. The tilt angle cited in the literature was confirmed by an independent structure determination (Supporting Information).
- (34) As described in ref 13a, Green has calculated the degree of strain imposed by tilting Cp ligands in [*n*]metallocenophanes for ferrocene and confirmed that an α angle of 0° is the most stable arrangement for ruthenocene. However, quantitative comparisons of the strain enthalpies of **1**, **10**, **15**, and **16** including the effect of the bridging atoms have not been reported, and thus it must be noted that the relationship between ring strain and ring tilt is accordingly a *qualitative* one. A lower temperature reported for the thermal ROP of the [2]ruthenocenophane **15** [α = 29.6(5)°, T_{onset} = 220 °C]³² compared to that of the [2]ferrocenophane **10** [α = 21.6(4)°, T_{onset} = 300 °C]^{28b} reflects this comparison.

Discussion

The differences in reactivity observed with $[n]$ metallocenophanes in the presence of P donors appear to be a consequence of the intricate combination of ring strain, metal–Cp bond strength, and metal–phosphine bond strength occurring within each system. Moderately strained [1]- and [2]ferrocenophanes [$\alpha = 20.8(5)^\circ$, **1** and $21.6(4)^\circ$, **10**] are inert toward P donors under ambient conditions but react with irradiation to give mixed hapticity bis(cyclopentadienyl) metallocycles, ring-opened monomeric zwitterions, or polyferrocenes. The photocontrolled reactivity of sila[1]ferrocenophanes has been previously exploited to provide mild routes to metallocopolymers with narrow molecular weight distributions.¹⁷ Highly tilted and strained [2]ruthenocenophanes [$\alpha = 29.6(5)^\circ$, **15** and $\alpha = 31.1^\circ$, **16**] react with P donors without irradiation to yield ring-slipped products **17–19**.

The difference in strain energies associated with the larger tilt angles in $[n]$ ruthenocenophanes compared to $[n]$ ferrocenophanes with the same *ansa* bridge is a consequence of the larger covalent radius of ruthenium. Despite lower ring strain, $[n]$ ferrocenophanes readily generate a pendant Cp anion to initiate photocontrolled ROP. The reactivity of $[n]$ ruthenocenophanes with P donors, however, is arrested after slippage to η^1 -coordination of a Cp ligand, which suggests more stable M– η^1 -Cp σ bonds.^{3d,35}

When ring strain is not an issue, as in the heteroleptic complex **13**[BPh₄] or a zwitterionic polymer chain (e.g., **8**), iron-bound PR₃ ligands were found to be readily substituted by a Cp anion with irradiation. Though rare, several examples of phosphine photolabilization have been previously reported.³⁶ This result provides an interesting parallel to the thermal retroconversion of slipped Cp ligands back to η^5 -coordination with displacement of a chelating phosphine, which occurs despite the enthalpic penalty of re-forming a strained ring. Both cases suggest an increased stability for homoleptic bonding arrangements over mixed sets of ligands.³⁷

The thermal reversibility of Cp haptotropic shifts with loss of the chelating dppe ligand from the SiMe₂-bridged **5** is attributed to the loosely bound P donor, which (unlike that in **6** or **11**) slowly dissociates in donor solvents at 25 °C. In contrast, in **11** the electron-donating ethane bridge promotes the strong coordination of the σ -bound Cp ligand relative to the case of **6**, creating a more robust metallocycle. The difference in the electronic features of the Cp ligand explains why, unlike **1**, the ethane-bridged [2]ferrocenophane **10** does not react with dppe: because of a less electrophilic metal center as a result of more electron-donating Cp ligands than those in **1**. Thus, unlike in silyl-bridged **6**, the η^1 -Cp ring of **11** resists dissociation from the metal center and contributes to the reversibility of eq 6. Direct comparison of Fe–C_{ipso} bond lengths in the solid state

is hampered by the fact that the metal-bound *ipso* carbon in **5** is sp² hybridized, while those in **6** and **11** are sp³ hybridized (Figures 3, 5, and 7). However, the Fe–C_{ipso} bond distance connecting the metal center and η^1 -Cp ring in **6** is notably long [**5**, 2.015(2) Å; **6**, 2.249(9) Å; **11**, 2.201(5) Å], consistent with an easily dissociable η^1 -Cp ligand.³⁸

The steric and electronic characteristics of P donors exert a subtle influence on the photochemical reactions with **1** or **10**. With **1**, partial displacement of a π -bound Cp ligand to produce a ring-slipped product is observed with both dmpe and the more sterically imposing dppe. The phenyl substituents restrict fluxional behavior in **5** to a greater extent than in **6** or **11**, as is apparent in the multinuclear NMR spectra. Interestingly, the weakly bound dppe does not remain coordinated to the iron center in the presence of dmpe, while **6**, with a more strongly coordinated dmpe ligand, reacts with one donor site of a second dmpe ligand with the loss of the σ -bound Cp ring to yield the zwitterion **7**. The dissociative mechanism proposed to operate when **5** exchanges a dppe ligand for dmpe to form **6** is consistent with the relatively stable (η^5 , η^1) coordination of the two Cp ligands in the 18-electron complex, **5**. Notably, while the dppe ligand in **5** readily dissociates in donor solvents and in the presence of dmpe, the stability of dmpe coordination in **6** provides a convenient entry into the mechanistic manifold for thermal ROP (Scheme 1). Interestingly, ROP in this case appears to be entropy-driven, kinetically facilitated by the lability of a weakly bound Cp ring, and not by release of significant ring-strain. To date, few examples of ROP involving strain-free monomers have been reported.³⁹

Concluding Remarks

A systematic study into the influence of ring-strain on the haptotropic flexibility of Cp ligands in [1]- and [2]metallocenophanes has been performed. Reactions with bidentate P donors revealed thermally reversible, photocontrolled haptotropic shifts of a Cp ligand from η^5 - to η^1 -coordination in moderately strained [1]- and [2]ferrocenophanes **1** and **10**. The highly strained [2]ruthenocenophanes **15** and **16** react without photoinitiation to produce similar ring-slipped products. Interestingly, though the [2]ruthenocenophanes react with P donors under milder conditions, the reactivity of the Cp ligands is arrested at the σ -bound complexes, whereas a Cp ligand can be fully substituted in **1** and **10** by P donors, promoting ROP.

Despite the anticipated affinity of the iron center in [1]- and [2]ferrocenophanes for monodentate phosphines, only macrocycles and cyclic polymers were observed from photolytic ROP initiated by PMe₃ or PPh₃, which suggests that pendant Cp anions can react with phosphine-substituted metal centers at the other end of a polymer chain. Controlled stoichiometric substitution of the three iron-bound PMe₃ ligands of **13**[BPh₄] by a Cp[−] anion was found to occur only with irradiation.

(35) For a recent computational analysis of M–C bonds (M = Fe or Ru) see: (a) Krapp, A.; Pandey, K. K.; Frenking, G. *J. Am. Chem. Soc.* **2007**, *129*, 7596. (b) Ehlers, A. W.; Frenking, G. *Organometallics* **1995**, *14*, 423.

(36) (a) Davies, S. G.; Metzler, M. R.; Watkins, W. C.; Compton, R. G.; Booth, J.; Eklund, J. C. *Perkin Trans.* **1993**, 1005. (b) Davies, S. G.; Metzler, M. R.; Yanada, K.; Yanada, R. *Chem. Commun.* **1993**, 658. (c) Aplin, R. T.; Booth, J.; Compton, R. G.; Davies, S. G.; Jones, S.; McNally, J. P.; Metzler, M. R.; Watkins, W. C. *Perkin Trans.* **1999**, 913.

(37) (a) [CpFeP₃]⁺ cations have been reported. See: Edwards, P. G.; Malik, K. M. A.; Ooi, L.; Price, A. J. *Dalton Trans.* **2006**, 433. (b) For a recent report discussing the stability of heteroleptic (Cp, N-donor) Fe complexes, see: Chan, W. Y.; Lough, A. J.; Manners, I. *Chem.–Eur. J.* **2007**, *13*, 8867 and ref 25b.

(38) At 2.249(9) Å, the Fe–C_{ipso} (η^1 -Cp) distance in **6** is particularly long for a localized Fe–C(sp³) bond (cf. all Fe–C bond distances greater than 2.2 Å found in the Cambridge Structural Database involved allylic moieties or bridging carbonyl groups). Typical Fe–C_{sp³} or Fe–C_{sp²} single bonds have been reported in the range of 2.0–2.1 Å. See: (a) Johnson, M. D. In *Comprehensive Organometallic Chemistry*; Wilkinson, G.; Stone, F. G. A., Abel, E. W., Eds.; Pergamon Press: Oxford, U.K., 1982; p 331. It also should be noted that recent attempts at the ROP of the spirocyclic 1-sila-3-ferracyclobutane (dppe)Fe(η^5 -C₅H₄SiMe₂CH₂) were unsuccessful. In this compound, the σ -bound CH₂–Fe distance was found to be 2.134(4) Å. See: (b) Kumar, M.; Cervantes-Lee, F.; Sharma, H. K.; Pannell, K. H. *Organometallics* **2007**, *26*, 3005.

(39) Cho, Y.; Baek, H.; Sohn, Y. S. *Macromolecules* **1999**, *32*, 2167.

The new chemistry reported here may be of broad generality. Interesting potential extensions can be envisaged to analogous species with different transition metals, bridging groups, and π -hydrocarbon rings, of which many new examples have been recently reported.^{8b,10g-r} Additionally, the ROP of the strain-free complex **6** offers a potential route for preparing organo-metallic polymers from unstrained monomers. The results outlined may also allow for new catalytic processes by photo-induced haptotropic shifts of Cp ligands.

Acknowledgment. We thank Dr. George R. Whittell for helpful discussions, Dr. Anne Staubitz, Dr. Craig P. Butts, and Dr. Tim Burrow for assistance with 2D NMR spectroscopy, Laurent Chabanne for MALDI-TOF MS, and Vivienne Black-

stone for collecting GPC data. I.M. thanks the European Union for a Marie Curie Chair and the Royal Society for a Wolfson Fellowship. D.E.H. thanks the Natural Sciences and Engineering Research Council of Canada for postgraduate scholarships.

Supporting Information Available: Detailed experimental section including syntheses and characterization of the compounds presented, selected ³¹P{¹H} and ¹H NMR spectra, X-ray crystallography experimental procedures, and CIF files for X-ray structures of compounds **5**, **6**, **11**, **13b**[BPh₄], **14**, and **16–19**. This material is available free of charge via the Internet at <http://pubs.acs.org>.

JA077334+